View metadata, citation and similar papers at core.ac.uk

brought to you by CORE

provided by Constellation

Muscle RANK is a key regulator of calcium storage, SERCA activity, and function of fast-twitch skeletal muscles

Sébastien S. Dufresne[1*], Nicolas A. Dumont[1*], Antoine Boulanger-Piette[1], Val A. Fajardo[2], Daniel Gamu[2], Sandrine-Aurélie Kake-Guena[3], Rares Ovidiu David[1], Patrice Bouchard[1], Éliane Lavergne[1], Josef M. Penninger[4], Paul C. Pape[3], A. Russell Tupling[2] and Jérôme Frenette[1,5]

[1] Centre Hospitalier Universitaire de Québec–Centre de Recherche du Centre Hospitalier de l'Université Laval (CHUQ-CRCHUL), Université Laval, Quebec City, QC, Canada G1V 4G2

[2] Department of Kinesiology, University of Waterloo, Waterloo, Ontario, Canada N2L 3G1

[3] Département de physiologie et biophysique, Université de Sherbrooke Faculté de Médecine et des Sciences de la Santé, Sherbrooke, Québec, Canada J1H 5N4

[4] IMBA, Institute of Molecular Biotechnology of the Austrian Academy of Sciences, 1030 Vienna, Austria

[5] Département de Réadaptation, Faculté de Médecine, Université Laval, Quebec City, QC, Canada G1V 4G2

*These authors contributed equally to this work

Running head: Rank is a novel calcium regulator in skeletal muscle

Keywords: RANK, skeletal muscle, SERCA

Copyright © 2016 by the American Physiological Society.

Corresponding author: Jérôme Frenette PT, Ph.D
CHUQ-CRCHUL
2705 boulevard Laurier, RC-9500
Quebec City, QC, Canada G1V 4G2
Phone: (418) 656-4141, ext. 47779
Fax: (418) 654-2145
E-mail: jerome.frenette@crchul.ulaval.ca

Abstract

Receptor-activator of nuclear factor kB (RANK), its ligand RANKL and the soluble decoy receptor osteoprotegerin (OPG) are the key regulators of osteoclast differentiation and bone remodeling. Here we show that RANK is also expressed in fully differentiated myotubes and skeletal muscle. Muscle RANK deletion (*RANK*^{mko}) has inotropic effects in denervated, but not in sham, extensor digitorum longus (EDL) muscles preventing the loss of maximum specific force while promoting muscle atrophy, fatigability and increased proportion of fast-twitch fibers. In denervated EDL muscles, RANK deletion markedly increased stromal interaction molecule 1 (Stim1) content, a calcium sensor, and altered activity of the sarco(endo)plasmic reticulum Ca^{2+} ATPase (SERCA) modulating Ca^{2+} storage. Muscle RANK deletion had no significant effects on the sham or denervated slow-twitch soleus (Sol) muscles. These data identify a novel role for RANK as a key regulator of calcium storage and SERCA activity, ultimately affecting denervated skeletal muscle function.

Introduction

Receptor-activator of nuclear factor kB ligand (RANKL), the membrane receptor RANK and the soluble decoy receptor osteoprotegerin (OPG) are members of the tumor necrosis factor (TNF) superfamily that regulate bone remodelling (26, 29). RANK/RANKL interaction activates Ca^{2+}-dependent and NF-kB signalling pathways, which affect osteoclast differentiation, activation and survival (29). The third protagonist, OPG, binds to RANKL and inhibits the RANK/RANKL interaction and subsequent osteoclastogenesis (46, 55). In addition to bone, RANK/RANKL has been detected in other tissues such as thymus, heart, kidney, liver, brain, blood vessels and skeletal muscles (17, 32, 51). The RANK/RANKL pathway is known to be involved in a variety of physiological and pathological conditions such as lymph-node organogenesis, formation of lactating mammary gland, breast cancer, central thermoregulation, T-cell/dendritic cell communication, vascular calcification, and bone metastasis (18, 36, 38, 41, 45).

Muscle hypertrophy/atrophy and gain/loss of bone mineral density occur in parallel in many physiological or pathological conditions and endocrine, mechanical factors, inflammatory and nutritional states affect simultaneously skeletal muscle and bone metabolism (3, 4, 16, 22, 39). These observations are consistent with the view that skeletal muscle and bone share common cell signalling pathways. For example, the Wnt/β-catenin signalling pathway is a major regulator of bone mass and muscle development and growth (24). Conditional deletion of *Ctnnb1* gene in osteocytes, which encodes for β-catenin, leads to impaired bone maturation and mineralization with increased RANKL:OPG ratio (27). In bone, RANKL/RANK interactions activate tumour necrosis factor receptor-associated factors 6 (TRAF-6), which subsequently induces the activation of downstream signalling molecules and intracellular calcium concentration ($[Ca^{2+}]_i$) oscillations (53). The ATP-dependent Ca^{2+}

pump, sarco(endo)plasmic reticulum Ca^{2+}ATPase (SERCA), is essential for $[Ca^{2+}]_i$ oscillations and plays a critical role in osteoclastogenesis (54). Moreover, it has been shown that TRAF-6 is required for functional bone resorption and muscle-specific TRAF-6 deletion preserves function and reduces atrophy in a model of muscle wasting indicating that TRAF-6 is an important regulator of both bone and muscle masses (19, 49, 50). Thus, common signalling pathways are emerging to explain the synchronicity between bone and skeletal muscle physiology and pathophysiology.

Muscle contraction involves the depolarization of the transverse-tubular (t) system, which activates dihydropyridine receptors (DHPRs) opening ryanodine receptor/Ca^{2+} release channels (RYR1) in the sarcoplasmic reticulum (SR) membrane. This results in the rapid influx of Ca^{2+} into the cytoplasm through RYR1 and binding of Ca^{2+} ions to troponin C causing the formation of actin-myosin cross-bridges and force development (34). Calcium reuptake in the SR is a tightly control mechanism mediated almost exclusively by SERCA-1a in fast-twitch fibers and SERCA-2a in slow-twitch fibers. The regulation of Ca^{2+} is also implicated in other physiological processes such as the maintenance and adaptation of muscle phenotypes (7, 40), while chronic rise in $[Ca^{2+}]_i$ is associated with different pathological states including muscle dystrophy (1) and the triggering of apoptotic processes (12, 42). Therefore, the appropriate regulation of $[Ca^{2+}]_i$ is a requirement for proper cell function, phenotype and survival.

We recently reported that OPG treatments protect against muscular dystrophy suggesting a potential role for RANK/RANKL/OPG pathway in muscle disease. In addition, muscle specific TRAF-6 deletion prevented muscle atrophy and decreased the expression of ubiquitin-proteasome components in models of denervation or starvation (28, 50). In the

present study, we hypothesized that muscle RANK, a receptor upstream of TRAF-6, is an important regulator of denervated muscle function. We report that RANK/RANKL regulates Ca^{2+} storage, function and phenotype, confirming a role for RANK in denervated skeletal muscles.

Material & Methods

Ethical Approval: All procedures were approved by the Université Laval Research Center Animal Care and Use Committee based on Canadian Council on Animal Care guidelines.

Animals: Mice carrying the $RANK^{floxed}$ or $RANK^{del}$ alleles and muscle creatine kinase-Cre (mck-Cre) mice were backcrossed five times to a C57BL/10J background before generating a specific RANK skeletal muscle deletion, the mck-Cre $RANK^{del/floxed}$, hereafter named $Rank^{mko}$ mice (18). $RANK^{mko}$ mice are viable, healthy and appeared indistinguishable from control $RANK^{floxed/floxed}$ mice that do not carry the Cre recombinase, hereafter named $RANK^{f/f}$ mice. Male wild-type (C57BL/10J) mice were purchased from the Jackson Laboratory and bred at our animal facility. Mice were screened for the desired genotype by PCR analysis. Food and water were provided ad libitum. At the end of the different experimental procedures, the mice were euthanized by cervical dislocation under anaesthesia.

Denervation: Sciatic denervation was performed under anaesthesia with isoflurane inhalation on adult mice aged between 12-18 weeks. Briefly, the hindlimbs were shaved and a small 0.5-cm incision was made proximal to the hip on the lateral side of the leg to expose and section a 3-5 mm piece of the sciatic nerve. The wounds were then closed with surgical sutures. The same surgery procedures were executed without sciatic denervation for sham mice. Mice were euthanized 14 days after sham or denervation procedures. Animals without chirurgical procedures were used as control mice.

Cell culture: C2C12 myoblasts (ATCC) were cultured in high glucose DMEM (HyClone) supplemented with 10% FBS (HyClone) and 1% antibiotic-antimycotic (Life Technologies)

150 in 5% CO_2 and at 37°C. When the myoblasts reached 90% confluence, the medium was
151 replaced by high glucose DMEM containing 1% FBS for 5 days to allow the myoblasts to
152 differentiate into myotubes (11).
153
154 **Genomic DNA for genotyping:** Genomic DNA from mouse tail tissue samples was isolated
155 and amplified by PCR. RANK, cre, and dystrophin was identified by isolating genomic DNA
156 from tail tissue and screening for the mutation or presence of the transgene by PCR. To detect
157 *delta*, *flox* and *wild-type* alleles primers used were p87, p88 and p105. Conditions : 94 ^{o}C 2
158 min, 40 cycles of (94 ^{o}C 30 s, 60 ^{o}C 20 s, 72 ^{o}C 1 min) and 72 ^{o}C 4 min. To detect the
159 presence of the *mck-cre* primers used were ALP 130 and ALP 131. Conditions : 94 ^{o}C 2 min,
160 40 cycles of (94 ^{o}C 30 s, 58 ^{o}C 10 s, 72 ^{o}C 1 min) and 72 ^{o}C 4 min. To detect *mdx* allele
161 primers used were p9427 and p259E. Conditions : 94 ^{o}C 3 min, 45 cycles of (94 ^{o}C 30 s, 57
162 ^{o}C 30 s, 72 ^{o}C 20 s) and 72 ^{o}C 10 min.

163 **Isometric contractile properties:** Mice were injected with buprenorphine (i.p. 0.1 mg/kg)
164 and anesthetised with pentobarbital sodium (i.p. 50 mg/kg) 15 min later. Mice were weighed
165 and the soleus (Sol) and extensor digitorum longus (EDL) muscles were carefully dissected,
166 attached to an electrode and a force sensor (305B-LR, Aurora Scientific, Inc.) to assess
167 contractile properties as described previously (9, 44). Muscle fatigability was examined by
168 stimulating muscle for 200 ms every second at 50 Hz until muscles lost 30% (Sol) or 50%
169 (EDL) of their initial force. Lastly, muscle length was measured, tendons were removed and
170 muscles weighed for calculation of muscle cross-sectional area and specific force (13).
171 Functional measurements were analyzed with the Dynamic Muscle Data Analysis software
172 (Aurora Scientific, Inc.).
173
174 **Immunohistochemistry:** Transversal Sol and EDL muscle sections (10 μm) were cut (Leica

Microsystems CM1850, Nussloch, Germany) in duplicate from the proximal and distal portions of the muscles. Sections were incubated overnight at 4°C with the following primary antibodies: anti-SERCA1a (Abcam), anti-SERCA2a (Abcam), anti-MyHC I (Novus Biological), anti-MyHC IIA (SC-71, DSHB), anti-MyHC IIB (BF-F3, DSHB), anti-MyHC IIX (6H1, DSHB), anti-dystrophin (NCL-Dys1, Vector Laboratories) and anti-RANK (R&D Systems). Pan-MyHC II was obtained by combining three antibodies: anti-MyHC IIA, anti-MyHC IIB and anti-MyHC IIX (DSHB). Fiber-type differentiation by myosin immunohistochemical was performed as described by Schiaffino et al. (43). Biotinylated secondary antibodies for immunohistochemistry were purchased from Vector Laboratories and Alexa Fluor® secondary antibodies from Invitrogen. The localization of RANK and dystrophin in the sarcolemmal membrane of skeletal muscles was determined by confocal microscopy. Briefly, confocal series were acquired using a Quorum WaveFX spinning disc confocal system (Quorum Technologies, Guleph, Ontario) with 491 nm and 561 nm solid state laser lines for excitation of green and red (Alexa-488 and Alexa-594), combined with appropriate BrightLine single-bandpass emission filters (536/40 nm and 624/40 nm, Semrock). For DAPI visualization, wide-field z-series were acquired at the same time with a DAPI fluorescence filter cube (Chroma Technology). The CCD camera used to capture the images was a Hamamatsu ImagEM C-9100.

Western blotting: Myotubes or skeletal muscles were homogenized in a lysis buffer containing 10 µl of protease inhibitor cocktail (Sigma-Aldrich). Protein homogenates were electrophoretically separated on SDS-polyacrylamide gels and transferred to polyvinylidene difluoride membranes (PVDF; Bio-Rad), blocked in 5% skim milk and incubated overnight at 4°C. The following primary antibodies (all from Santa Cruz Biotechnology) were used: anti-SERCA-1a, anti-SERCA-2a, anti-Stim1, anti-calsequestrin, and anti-RANK anti-

GAPDH. The membranes were washed and incubated with appropriate HRP-conjugated secondary antibodies (Santa Cruz Biotechnology). Protein bands were revealed using the ECL-Plus chemiluminescent detection system (Perkin-Elmer). Films (Denville scientific inc.) were used to detect a chemiluminescent signal, scanned, and analyzed using Quantity One software (v4.6.6, Bio-Rad) (10).

Calcium measurements: In another set of experiments, the concentration of total Ca^{2+} in Sol and EDL muscles was determined using the Ca^{2+}-dependent UV absorbance of 1,2-Bis (2-Aminophenoxy) ethane-*N,N,N',N'*-tetraacetic acid (BAPTA) which is a good estimate of [CaT] in the SR (30). Briefly, whole Sol and EDL muscles from 12 week-old mice were weighed and homogenized in a solution containing 0.3 mM BAPTA and sodium dodecyl sulphate (SDS) detergent to dissolve the surface and SR membranes. The mixture was then centrifuged removing proteins and other insoluble muscle components to prevent unwanted absorbance or light scattering. To determine the amount of total Ca^{2+}, the supernatant was divided into four aliquots for separate absorbance measurements taken at 292 nm: 1) the supernatant alone; 2) The UV absorbance spectrum (240-390 nm) of the supernatant plus 1 mM EGTA added to give a zero Ca^{2+} BAPTA spectrum; 3) the supernatant with a known amount of Ca^{2+} standard added; and 4) the supernatant with excess Ca^{2+} added to complex essentially all of the binding sites on BAPTA with Ca^{2+}. From the absorbance data and the equations given by Lamboley et al. (30), values of total Ca^{2+} concentration were estimated and reported here in units of mmoles/kg muscle weight. [CaT] measurements include the following components: extracellular ($[CaT]_{EC}$), intracellular outside of the SR ($[CaT]_{NonSR}$), and intracellular inside the SR ($[CaT]_{SR}$). The Ca^{2+} chelator, BAPTA, should provide the best estimate of $[CaT]_{SR}$ under physiological conditions (30).

SERCA parameters: Homogenates from the muscles of WT and KO mice were used to

225 determine Ca^{2+} dependent Ca^{2+}-ATPase activity using a spectrophotometric assay
226 (SPECTRAmax Plus; Molecular Devices) (47). Briefly, reaction buffer (200 mM KCl, 20
227 mM HEPES (pH 7.0), 15 mM $MgCl_2$, 1 mM EGTA, 10 mM NaN_3, 5 mM ATP and 10 mM
228 PEP) containing 18 U/mL of both LDH and PK, as well as the homogenate were added to test
229 tubes containing 15 different concentrations of Ca^{2+}, ranging between 7.6 and 4.7 pCa units
230 in the presence and absence of ionophore A23187 (4.2 μM). In the absence of the ionophore,
231 Ca^{2+} accumulates inside the SR vesicle and causes back-inhibition of SERCA pumps, which
232 is more relevant to the physiological system found in skeletal muscle. Aliquots (100 μl) were
233 then transferred in duplicate to a clear bottom 96-well plate (Costar, Corning Incorporated,
234 NY), where 0.3 mM NADH was added to start the reaction. The plate was read at a
235 wavelength of 340 nm for 30 min at 37°C. The different concentrations of Ca^{2+} in the wells
236 were used to determine the maximal enzyme activity (Vmax) and pCa50, which is defined as
237 the $[Ca^{2+}]f$ required to achieve 50% of Vmax. Lastly, cyclopiazonic acid (CPA; 40 μM), a
238 highly specific SERCA inhibitor, was used to determine background activity which was
239 subtracted from the total Ca^{2+}-ATPase activity measured in muscle homogenate. All data
240 were then plotted against the negative logarithm of $[Ca^{2+}]f$ (pCa) using basic statistatical
241 software (GraphPad PrismTM version 4) to determine Vmax and pCa50. pCa50 was
242 determined by non-linear regression curve fitting using the sigmoidal dose response.
243
244 **Statistical analyses.** All values are expressed as means ± SEM. The data were analyzed with
245 Student's t-test, Chi-square test or one-way ANOVA followed by a Tukey's test (InStat). The
246 levels of significance were set at * $p<0.05$, ** $p<0.01$, *** $p<0.001$ for genotype ($RANK^{f/f}$ vs
247 $RANK^{mko}$) or # $p<0.05$ for treatment (Sham vs Den).
248
249
250

Results

RANK is expressed in fully differentiated C2C12 myotubes and at the sarcolemmal membrane of skeletal muscle

To assess RANK expression in muscle cells, we first analysed its expression in C2C12 myoblasts and differentiated myotubes. RANK was found to be expressed in C2C12 myotubes but not in proliferating C2C12 myoblasts (Fig. 1a). We next analysed RANK expression in skeletal muscle cells *in situ* using confocal microscopy. Confocal immunofluorescence confirmed the presence of RANK protein on the membrane of fast-twitch (EDL) (Fig. 1b) and slow-twitch (Sol; data not shown) skeletal muscle fibers. To confirm specific RANK expression in muscle, we crossed $RANK^{f/f}$ mice onto a muscle creatine kinase-Cre background to generate muscle-specific RANK knockout mice ($RANK^{mko}$ mice). PCR results validated the deletion of the RANK allele specifically in skeletal muscle tissue and partially in heart (Fig. 1c). Deletion efficiency was confirmed at the protein level in skeletal muscles where RANK immunostaining was not detectable (Fig. 1b).

RANK deletion affects denervated muscle mass and function

To examine the role of RANK/RANKL in muscle pathophysiology, muscle mass, contractile properties and fiber type proportions were examined in sham and denervated Sol and EDL muscles from $RANK^{f/f}$ and $RANK^{mko}$ mice. Denervation and/or RANK deletion did not influence mouse body weight. Treatment, but not genotype, reduced EDL and Sol muscle masses when normalized to body weights (Table 1). Intriguingly, denervated EDL muscles from $RANK^{mko}$ mice exhibited inotropic effects as determined by the decrease in muscle mass (Fig. 2a), combined with the partial preservation of maximum specific force (sP_0; N/cm^2) compared to denervated $RANK^{f/f}$ muscles (Fig. 2b). The absolute force production (P_0; g) was not different between $RANK^{f/f}$ and $RANK^{mko}$ EDL muscle but RANK deletion prevented the

loss of twitch tension (P_t) in denervated EDL muscles (Table 2). The contractile properties of control mice were similar between both genotypes (Table 2). Lastly, the P_t/P_0 ratio was increased in both Sol and EDL muscles of denervated *RANK*^{mko} mice (Fig. 2c), suggesting a change in myofilament Ca^{2+} sensitivity and/or SR Ca^{2+} release.

Denervation led to decreased fatigue resistance in both Sol and EDL muscles during a repetitive and glycolytic fatigue protocol (Fig. 2d,e). Both sham and denervated *RANK*^{mko} EDL muscles exhibited increased fatigability compared to sham and denervated *RANK*$^{f/f}$ muscles (Fig. 2d,e). In accordance with the higher fatigability, immunohistochemical fiber typing showed that the slow-twitch fibers were nearly absent in sham *RANK*^{mko} EDL muscles while the proportion of fast-twitch fibers (IIA+IIX+IIB) was significantly increased in denervated *RANK*^{mko} EDL muscles compared to denervated *RANK*$^{f/f}$ EDL muscles (Fig. 2f). The proportion of fiber type over 100% in denervated *RANK*^{mko} EDL muscles indicated the presence of hybrid fibers expressing multiple isoforms of MyHC. No changes in muscle fiber type were observed in Sol muscles (Fig. 3a) indicating that the impact of muscle RANK deletion on muscle fatigue and phenotype is limited to fast-twitch EDL muscles. Noticeably, the proportion of fast-twitch fibers expressing SERCA-1a was reduced and the proportion of fast-twitch fibers expressing SERCA-2a was increased in RANK^{mko} Sol and EDL muscles (Fig 3b).

Total calcium and SERCA activity and expression in RANK $^{f/f}$ and RANK^{mko} muscles

Our recent published data show an inverse relationship between [CaT] and muscle mass, where the highest values of [CaT] are seen with the lowest muscle weights (30). Since RANK deletion promotes muscle atrophy and prevents force deficits in denervated muscles, we next measured [CaT] in EDL muscles (Fig. 4a-c). Despite similar muscle masses, the

301 average values of [CaT] were 42% lower in sham *RANK*^{mko} relative to sham *RANK*$^{f/f}$ EDL
302 muscles (Fig. 4c), indicating that under non pathological conditions muscle RANK is
303 important in Ca^{2+} storage of skeletal muscles. Consistent with the observed inverted
304 relationship between [CaT] and muscle weights, we found that muscle weights below <4.5
305 mg had much greater [CaT] than the bigger muscles, but data were non-linear due to a floor
306 effect in the assay (Fig. 4b). Consistent with the reduced muscle mass in denervated *RANK*^{mko}
307 EDL muscles (Fig. 2a), [CaT] increased by 93% in denervated *RANK*^{mko} EDL muscles while
308 it did not significantly increase in denervated *RANK*$^{f/f}$ EDL muscles (Fig. 4c).
309
310 Since SERCA is critical for Ca^{2+} cycling in the SR, we analyzed SERCA1a and SERCA2a
311 expression and SERCA activity in Sol and EDL muscle extracts. Western blotting analyses
312 show that SERCA1a content is significantly reduced in denervated muscles while SERCA2a
313 content is significantly increased following denervation, independently of the genotype (Fig
314 4d). No difference in calsequestrin content, a calcium binding protein located in SR, was
315 observed between *RANK*$^{f/f}$ and *RANK*^{mko} muscles (Fig 4d). However, the content of the
316 stromal interaction molecule 1 (Stim1), which functions as a calcium sensor in the SR,
317 increased by 77% and 411% in denervated *RANK*$^{f/f}$ and *RANK*^{mko} EDL muscles, relative to
318 their respective sham (Fig 4d). The concentration of Stim1 increased significantly by 184%
319 in denervated *RANK*^{mko} compared to denervated *RANK*^{mko} EDL muscles. Next, we assessed
320 SERCA Ca^{2+}-dependent ATPase activity in muscle homogenates from sham and denervated
321 *RANK*$^{f/f}$ and *RANK*^{mko} Sol and EDL muscles over Ca^{2+} concentrations ranging from *p*Ca 7.0
322 to *p*Ca 4.5. Interestingly, upon denervation, maximal SERCA activity was reduced in both
323 the Sol and EDL muscles (Fig. 4e-g and Fig. 5). Moreover, maximal SERCA activity was
324 significantly reduced in both the sham and denervated *RANK*^{mko} EDL compared to the sham
325 and denervated *RANK*$^{f/f}$ EDL (Fig. 4c-f). This inhibitory effect of RANK deletion on SERCA

activity was limited to EDL muscles and did not affect Sol muscles. Overall, these findings demonstrate a direct role for muscle RANK in the regulation of SERCA activity and Stim1 content in fast-twitch EDL muscles.

Discussion

We previously demonstrated that systemic injection of OPG, the decoy receptor of RANKL, restores muscle force and improves muscle histology in dystrophic *mdx* mice (9). However, whether the RANK/RANKL/OPG system directly or indirectly affects skeletal muscle was unknown. In this paper, using muscle specific RANK mutant mice, we demonstrate that RANK is expressed in skeletal muscle cells where it directly regulates muscle function. Importantly, muscle-specific RANK deletion protects from denervation-induced loss of muscle force and modulates total Ca^{2+} storage and SERCA activity.

RANK is well characterized in osteoclasts where it leads to the activation of different signalling pathways, especially NF-kB and calcium-dependent pathways (5). In skeletal muscle, Ca^{2+} is a master regulator of multiple intracellular processes such as myosin-actin cross-bridging, protein synthesis and degradation, mitochondrial adaptation and fiber type shifting, through the control of Ca^{2+} sensitive proteases and transcriptional factors such as NFATc1 (2). Consistent with a role of RANK in the regulation of calcium handling, conditional deletion of *RANK* in skeletal muscle affected muscle contraction post-denervation, atrophy and fiber type, all of which are regulated by Ca^{2+} (2). Intriguingly, muscle-specific *RANK* deletion prevents the loss of specific force production but not the loss of muscle mass following denervation. Without significant changes in muscle mass, muscle strength can be altered by (1) the amplitude or duration of the Ca^{2+} transient or (2) the sensitivity of the myofilaments to Ca^{2+}. For instance, reduced force production in aged muscle is partially caused by reduced Ca^{2+} content and myofilament sensitivity (31). Our findings show that $RANK^{mko}$ denervated muscles have higher [CaT], which originates from increased intracellular calcium stocks (30, 33). Therefore, higher Ca^{2+} content potentially results in greater rates of Ca^{2+} release, increased myoplasmic Ca^{2+} transients, and, ultimately,

preserved muscle force production. These results are supported by the increased specific force and Pt/P_0 ratio in denervated *RANK*^{mko} EDL muscle, indicating that these muscles are able to generate a stronger contraction following submaximal stimulation.

The higher releasable Ca^{2+} content is not explained by greater SERCA activity since we found that denervated *RANK*^{mko} muscles had low SERCA activity rate compared to the denervated *RANK*$^{f/f}$. Moreover, we observed no change in CSQ content making it unlikely to explain the greater releasable Ca^{2+} content; however, in the normal EDL muscles it was shown that the resting SR Ca^{2+} content is only a relatively small proportion of its maximal content and that Ca^{2+} bound to CSQ is only one-third of its saturated level (14, 35, 52). Thus, it is likely that the increase in [CaT] observed in the denervated *RANK*^{mko} EDL reflects an increased binding of Ca^{2+} in the SR thereby increasing releasable SR Ca^{2+} and ultimately specific force production. In this respect, the relatively greater inhibition of SERCA activity may serve to prolong the Ca^{2+} transient and increase force production, while decreasing the fatigue resistance. Accordingly, we observed higher muscle strength following a single contraction (Pt) in denervated *RANK*^{mko} EDL muscle combined with increased fatigability following repeated maximal contractions. The exact mechanisms lowering SERCA activity in response to RANK deletion are unknown and require further investigation – and analysis of sarcolipin and phospholamban, two well-known regulators of the SERCA pump (15), indicate increased expression of both proteins in response to denervation, however no significant differences were found between genotype (data not shown).

Enhanced Ca^{2+} entry could be responsible for any increase in SR Ca^{2+} content in muscle. In osteoclasts, RANKL-mediated Ca^{2+} entry could arise from intracellular or extracellular origin (6, 25). Members of the transient receptor potential vanilloid channels (TRPV) family,

382 TRPV2 and TRPV5, were demonstrated to mediate RANKL-induced calcium entry (6, 23).
383 Store-operated calcium entry (SOCE) channels, that sense declining Ca^{2+} ion concentration in
384 the SR, were also associated with RANKL-induced calcium entry (23). For instance,
385 silencing of the SOCE channel Orai1 with specific shRNA inhibits RANKL-induced
386 osteoclastogenesis by suppressing NFATc1 induction (20). Mice lacking SOCE specifically
387 in skeletal muscle exhibit reduced muscle mass and increased susceptibility to fatigue
388 whereas $Stim1^{-/-}$ myotubes failed to refill their stores and altered expression of key SR
389 proteins (48). Furthermore, the use of SERCA inhibitor suggests that under some conditions
390 the role of SERCA in replenishing Ca^{2+} stores is limited (37). Our current findings that
391 denervation treatment and RANK deletion markedly increased Stim1 content (184%) may
392 explain, in part, the discrepancy between the rise in [CaT] and the depression of SERCA
393 activity in denervated $RANK^{mko}$ EDL muscles. It is thus tempting to speculate that SOCE
394 would compensate for the lack of SERCA activity in denervated $RANK^{mko}$ EDL muscles.
395 The mechanisms by which RANKL/RANK controls Ca^{2+} storage in skeletal muscle cells
396 requires further experiments, nevertheless our findings provide the first evidence that RANK
397 is a novel regulator of Ca^{2+} storage in skeletal muscle cells.
398
399 With respect to EDL muscle fatigability, we found that both denervation and RANK
400 deletion led to higher fatigability than their wild type and sham-operated counterparts.
401 Consistent with this observation, we found that $RANK^{mko}$ muscles increased the number of
402 fast-twitch type II fibers; however, the disproportionate increase of fatigability in $RANK^{mko}$
403 muscle compared to the relatively modest changes in fiber type and that no changes on
404 muscle contractility, fatigue and phenotype were observed in Sol muscles, suggests that the
405 muscle fiber type phenotype may not be the main reason to explain the fatigue in $RANK^{mko}$
406 muscle. Indeed, the decreased fatigue resistance observed following denervation was

associated with an increased proportion of type I fibres in both *RANK*$^{f/f}$ and *RANK*^{mko} Sol and EDL muscles. It could be speculated that the altered calcium signalling following muscle-specific *RANK* deletion impairs mitochondrial function given the well-established role of the calcium-dependent effectors calcineurin and NFATc1 in enhancing muscle endurance and mitochondrial respiratory capacity (21). Nevertheless, our findings indicate that RANK deletion enhances force production, promotes a fast-twitch phenotype and fatigability while increasing stim1 content and decreasing SERCA activity.

Perspective and conclusion

Osteoporosis and muscle wasting occur simultaneously in a variety of pathologies, although common signalling pathways between these two processes were not identified (Fig. 6). Here, we show that in addition to its role in bone homeostasis, RANK signalling also regulates Ca^{2+} storage, muscle mass, and muscle performance. Muscle-specific deletion of RANK has an inotropic effect on denervated fast-twitch EDL muscles, largely composed of type IIA, IIX, and IIB fibers. Fast-twitch fibers are usually the first to be affected in several forms of muscular and neuromuscular diseases and aging conditions, leading to premature loss of function and important incapacities (8). Our findings show for the first time that fast-twitch fibers may be specifically targeted to enhance their force production. Although these results are preliminary and the long-term effects remain to be determined, this discovery opens a whole new field of research and new therapeutics avenues for conditions affecting in synchrony bone and skeletal muscle and potentially heart diseases.

Disclosures section**:** J.F., S.S.D., N.A.D., and J.M.P. conceived the project and its design; S.S.D., N.A.D., P.B., A.B.P, V.A.F., D.G., S.A.K.G., O.D., R.T., P.C.P. and E.L. performed experiments and data analysis; J.F., S.S.D., and N.A.D. wrote the manuscript; and all authors checked for scientific content and approved the final manuscript. JF is supported by CIHR and NSERC and JMP by an advanced ERC grant and the Austrian academy of Sciences. The authors declare no competing interests.

1. **Allen DG**, **Gervasio OL**, **Yeung EW**, **Whitehead NP**. Calcium and the damage pathways in muscular dystrophy. *Can J Physiol Pharmacol* 88: 83–91, 2010.
2. **Berchtold MW**, **Brinkmeier H**, **Müntener M**. Calcium ion in skeletal muscle: its crucial role for muscle function, plasticity, and disease. *Physiol Rev* 80: 1215–1265, 2000.
3. **Bloomfield SA**. Changes in musculoskeletal structure and function with prolonged bed rest. *Med Sci Sports Exerc* 29: 197–206, 1997.
4. **Boss GR**, **Seegmiller JE**. Age-related physiological changes and their clinical significance. *West J Med* 135: 434–440, 1981.
5. **Boyle WJ**, **Simonet WS**, **Lacey DL**. Osteoclast differentiation and activation. *Nature* 423: 337–342, 2003.
6. **Chamoux E**, **Bisson M**, **Payet MD**, **Roux S**. TRPV-5 mediates a receptor activator of NF-kappaB (RANK) ligand-induced increase in cytosolic Ca2+ in human osteoclasts and down-regulates bone resorption. *J Biol Chem* 285: 25354–25362, 2010.
7. **Chin ER**. Role of Ca2+/calmodulin-dependent kinases in skeletal muscle plasticity. *J Appl Physiol Bethesda Md 1985* 99: 414–423, 2005.
8. **Ciciliot S**, **Rossi AC**, **Dyar KA**, **Blaauw B**, **Schiaffino S**. Muscle type and fiber type specificity in muscle wasting. *Int J Biochem Cell Biol* 45: 2191–2199, 2013.
9. **Dufresne SS**, **Dumont NA**, **Bouchard P**, **Lavergne É**, **Penninger JM**, **Frenette J**. Osteoprotegerin Protects against Muscular Dystrophy. *Am J Pathol* 185: 920–926, 2015.
10. **Dufresne SS**, **Frenette J**. Investigation of wild-type and mycolactone-negative mutant Mycobacterium ulcerans on skeletal muscle: IGF-1 protects against mycolactone-induced muscle catabolism. *Am J Physiol Regul Integr Comp Physiol* 304: R753–762, 2013.
11. **Dumont N**, **Frenette J**. Macrophages protect against muscle atrophy and promote muscle recovery in vivo and in vitro: a mechanism partly dependent on the insulin-like growth factor-1 signaling molecule. *Am J Pathol* 176: 2228–2235, 2010.
12. **Francini F**, **Formigli L**, **Meacci E**, **Vassalli M**, **Nosi D**, **Quercioli F**, **Tiribilli B**, **Bencini C**, **Squecco R**, **Bruni P**, **Orlandini SZ**. Ca+2 homeostasis and cytoskeletal rearrangement operated by sphingosine 1-phosphate in C2C12 myoblastic cells. *J Gravitational Physiol J Int Soc Gravitational Physiol* 9: P281–282, 2002.
13. **Frenette J**, **St-Pierre M**, **Côté CH**, **Mylona E**, **Pizza FX**. Muscle impairment occurs rapidly and precedes inflammatory cell accumulation after mechanical loading. *Am J Physiol Regul Integr Comp Physiol* 282: R351–357, 2002.
14. **Fryer MW**, **Stephenson DG**. Total and sarcoplasmic reticulum calcium contents of skinned fibres from rat skeletal muscle. *J Physiol* 493 (Pt 2): 357–370, 1996.
15. **Gamu D**, **Bombardier E**, **Smith IC**, **Fajardo VA**, **Tupling AR**. Sarcolipin provides a novel muscle-based mechanism for adaptive thermogenesis. *Exerc Sport Sci Rev* 42: 136–142, 2014.
16. **Goldspink DF**. The effects of denervation on protein turnover of the soleus and extensor digitorum longus muscles of adult mice. *Comp Biochem Physiol B* 61: 37–41, 1978.
17. **Hanada R**, **Hanada T**, **Sigl V**, **Schramek D**, **Penninger JM**. RANKL/RANK-beyond bones. *J Mol Med Berl Ger* 89: 647–656, 2011.
18. **Hanada R**, **Leibbrandt A**, **Hanada T**, **Kitaoka S**, **Furuyashiki T**, **Fujihara H**, **Trichereau J**, **Paolino M**, **Qadri F**, **Plehm R**, **Klaere S**, **Komnenovic V**, **Mimata H**, **Yoshimatsu H**, **Takahashi N**, **von Haeseler A**, **Bader M**, **Kilic SS**, **Ueta Y**, **Pifl C**, **Narumiya S**, **Penninger JM**. Central control of fever and female body temperature by RANKL/RANK. *Nature* 462: 505–509, 2009.

19. **Hindi SM**, **Sato S**, **Choi Y**, **Kumar A**. Distinct roles of TRAF6 at early and late stages of muscle pathology in the mdx model of Duchenne muscular dystrophy. *Hum Mol Genet* 23: 1492–1505, 2014.
20. **Hwang S-Y**, **Putney JW**. Orai1-mediated calcium entry plays a critical role in osteoclast differentiation and function by regulating activation of the transcription factor NFATc1. *FASEB J Off Publ Fed Am Soc Exp Biol* 26: 1484–1492, 2012.
21. **Jiang LQ**, **Garcia-Roves PM**, **de Castro Barbosa T**, **Zierath JR**. Constitutively active calcineurin in skeletal muscle increases endurance performance and mitochondrial respiratory capacity. *Am J Physiol Endocrinol Metab* 298: E8–E16, 2010.
22. **Jost PD**. Simulating human space physiology with bed rest. *Hippokratia* 12 Suppl 1: 37–40, 2008.
23. **Kajiya H**, **Okamoto F**, **Nemoto T**, **Kimachi K**, **Toh-Goto K**, **Nakayana S**, **Okabe K**. RANKL-induced TRPV2 expression regulates osteoclastogenesis via calcium oscillations. *Cell Calcium* 48: 260–269, 2010.
24. **Kohn AD**, **Moon RT**. Wnt and calcium signaling: β-Catenin-independent pathways. *Cell Calcium* 38: 439–446, 2005.
25. **Komarova SV**, **Pilkington MF**, **Weidema AF**, **Dixon SJ**, **Sims SM**. RANK ligand-induced elevation of cytosolic Ca2+ accelerates nuclear translocation of nuclear factor kappa B in osteoclasts. *J Biol Chem* 278: 8286–8293, 2003.
26. **Kong YY**, **Feige U**, **Sarosi I**, **Bolon B**, **Tafuri A**, **Morony S**, **Capparelli C**, **Li J**, **Elliott R**, **McCabe S**, **Wong T**, **Campagnuolo G**, **Moran E**, **Bogoch ER**, **Van G**, **Nguyen LT**, **Ohashi PS**, **Lacey DL**, **Fish E**, **Boyle WJ**, **Penninger JM**. Activated T cells regulate bone loss and joint destruction in adjuvant arthritis through osteoprotegerin ligand. *Nature* 402: 304–309, 1999.
27. **Kramer I**, **Halleux C**, **Keller H**, **Pegurri M**, **Gooi JH**, **Weber PB**, **Feng JQ**, **Bonewald LF**, **Kneissel M**. Osteocyte Wnt/beta-catenin signaling is required for normal bone homeostasis. *Mol Cell Biol* 30: 3071–3085, 2010.
28. **Kumar A**, **Bhatnagar S**, **Paul PK**. TWEAK and TRAF6 regulate skeletal muscle atrophy: *Curr Opin Clin Nutr Metab Care* 15: 233–239, 2012.
29. **Lacey D.**, **Timms E**, **Tan H-L**, **Kelley M.**, **Dunstan C.**, **Burgess T**, **Elliott R**, **Colombero A**, **Elliott G**, **Scully S**, **Hsu H**, **Sullivan J**, **Hawkins N**, **Davy E**, **Capparelli C**, **Eli A**, **Qian Y-X**, **Kaufman S**, **Sarosi I**, **Shalhoub V**, **Senaldi G**, **Guo J**, **Delaney J**, **Boyle W.** Osteoprotegerin Ligand Is a Cytokine that Regulates Osteoclast Differentiation and Activation. *Cell* 93: 165–176, 1998.
30. **Lamboley CRH**, **Kake Guena SA**, **Touré F**, **Hébert C**, **Yaddaden L**, **Nadeau S**, **Bouchard P**, **Wei-LaPierre L**, **Lainé J**, **Rousseau EC**, **Frenette J**, **Protasi F**, **Dirksen RT**, **Pape PC**. New method for determining total calcium content in tissue applied to skeletal muscle with and without calsequestrin. *J Gen Physiol* 145: 127–153, 2015.
31. **Lamboley CR**, **Wyckelsma VL**, **Dutka TL**, **McKenna MJ**, **Murphy RM**, **Lamb GD**. Contractile properties and sarcoplasmic reticulum calcium content in type I and type II skeletal muscle fibres in active aged humans. *J Physiol* 593: 2499–2514, 2015.
32. **Leibbrandt A**, **Penninger JM**. RANK/RANKL: regulators of immune responses and bone physiology. *Ann N Y Acad Sci* 1143: 123–150, 2008.
33. **Manno C**, **Ríos E**. A better method to measure total calcium in biological samples yields immediate payoffs. *J Gen Physiol* 145: 167–171, 2015.
34. **Melzer W**, **Herrmann-Frank A**, **Lüttgau HC**. The role of Ca2+ ions in excitation-contraction coupling of skeletal muscle fibres. *Biochim Biophys Acta* 1241: 59–116, 1995.
35. **Murphy RM**, **Larkins NT**, **Mollica JP**, **Beard NA**, **Lamb GD**. Calsequestrin

content and SERCA determine normal and maximal Ca2+ storage levels in sarcoplasmic reticulum of fast- and slow-twitch fibres of rat. *J Physiol* 587: 443–460, 2009.
36. **Nagy V**, **Penninger JM**. The RANKL-RANK Story. *Gerontology* (February 14, 2015). doi: 10.1159/000371845.
37. **Okubo Y**, **Suzuki J**, **Kanemaru K**, **Nakamura N**, **Shibata T**, **Iino M**. Visualization of Ca2+ Filling Mechanisms upon Synaptic Inputs in the Endoplasmic Reticulum of Cerebellar Purkinje Cells. *J Neurosci* 35: 15837–15846, 2015.
38. **Page G**, **Miossec P**. RANK and RANKL expression as markers of dendritic cell-T cell interactions in paired samples of rheumatoid synovium and lymph nodes. *Arthritis Rheum* 52: 2307–2312, 2005.
39. **Pang MYC**, **Eng JJ**, **McKay HA**, **Dawson AS**. Reduced hip bone mineral density is related to physical fitness and leg lean mass in ambulatory individuals with chronic stroke. *Osteoporos Int J Establ Result Coop Eur Found Osteoporos Natl Osteoporos Found USA* 16: 1769–1779, 2005.
40. **Patterson MF**. Denervation produces different single fiber phenotypes in fast- and slow-twitch hindlimb muscles of the rat. *AJP Cell Physiol* 291: 518–528, 2006.
41. **Perlot T**, **Penninger JM**. Development and function of murine B cells lacking RANK. *J Immunol Baltim Md 1950* 188: 1201–1205, 2012.
42. **Sandri M**. Apoptotic signaling in skeletal muscle fibers during atrophy. *Curr Opin Clin Nutr Metab Care* 5: 249–253, 2002.
43. **Schiaffino S**, **Gorza L**, **Sartore S**, **Saggin L**, **Ausoni S**, **Vianello M**, **Gundersen K**, **Lømo T**. Three myosin heavy chain isoforms in type 2 skeletal muscle fibres. *J Muscle Res Cell Motil* 10: 197–205, 1989.
44. **Segal SS**, **Faulkner JA**. Temperature-dependent physiological stability of rat skeletal muscle in vitro. *Am J Physiol* 248: C265–270, 1985.
45. **Sigl V**, **Penninger JM**. RANKL/RANK - from bone physiology to breast cancer. *Cytokine Growth Factor Rev* 25: 205–214, 2014.
46. **Simonet W.**, **Lacey D.**, **Dunstan C.**, **Kelley M**, **Chang M-S**, **Lüthy R**, **Nguyen H.**, **Wooden S**, **Bennett L**, **Boone T**, **Shimamoto G**, **DeRose M**, **Elliott R**, **Colombero A**, **Tan H-L**, **Trail G**, **Sullivan J**, **Davy E**, **Bucay N**, **Renshaw-Gegg L**, **Hughes T.**, **Hill D**, **Pattison W**, **Campbell P**, **Sander S**, **Van G**, **Tarpley J**, **Derby P**, **Lee R**, **Boyle W.** Osteoprotegerin: A Novel Secreted Protein Involved in the Regulation of Bone Density. *Cell* 89: 309–319, 1997.
47. **Smith IC**, **Bombardier E**, **Vigna C**, **Tupling AR**. ATP consumption by sarcoplasmic reticulum Ca^{2+} pumps accounts for 40-50% of resting metabolic rate in mouse fast and slow twitch skeletal muscle. *PloS One* 8: e68924, 2013.
48. **Stiber J**, **Hawkins A**, **Zhang Z-S**, **Wang S**, **Burch J**, **Graham V**, **Ward CC**, **Seth M**, **Finch E**, **Malouf N**, **Williams RS**, **Eu JP**, **Rosenberg P**. STIM1 signalling controls store-operated calcium entry required for development and contractile function in skeletal muscle. *Nat Cell Biol* 10: 688–697, 2008.
49. **Sun H**, **Gong Y**, **Qiu J**, **Chen Y**, **Ding F**, **Zhao Q**. TRAF6 Inhibition Rescues Dexamethasone-Induced Muscle Atrophy. *Int J Mol Sci* 15: 11126–11141, 2014.
50. **Sun H**, **Qiu J**, **Chen Y**, **Yu M**, **Ding F**, **Gu X**. Proteomic and bioinformatic analysis of differentially expressed proteins in denervated skeletal muscle. *Int. J. Mol. Med.* (April 8, 2014). doi: 10.3892/ijmm.2014.1737.
51. **Theill LE**, **Boyle WJ**, **Penninger JM**. RANK-L and RANK: T cells, bone loss, and mammalian evolution. *Annu Rev Immunol* 20: 795–823, 2002.
52. **Trinh HH**, **Lamb GD**. Matching of sarcoplasmic reticulum and contractile properties in rat fast- and slow-twitch muscle fibres. *Clin Exp Pharmacol Physiol* 33:

591–600, 2006.
53. **Walsh MC**, **Choi Y**. Biology of the RANKLâ€“RANKâ€“OPG System in Immunity, Bone, and Beyond. *Front Immunol* 5, 2014.
54. **Yang Y-M**, **Kim MS**, **Son A**, **Hong JH**, **Kim K-H**, **Seo JT**, **Lee S-I**, **Shin DM**. Alteration of RANKL-Induced Osteoclastogenesis in Primary Cultured Osteoclasts From SERCA2 $^{+/-}$ Mice. *J Bone Miner Res* 24: 1763–1769, 2009.
55. **Yasuda H**, **Shima N**, **Nakagawa N**, **Yamaguchi K**, **Kinosaki M**, **Mochizuki S**, **Tomoyasu A**, **Yano K**, **Goto M**, **Murakami A**, **Tsuda E**, **Morinaga T**, **Higashio K**, **Udagawa N**, **Takahashi N**, **Suda T**. Osteoclast differentiation factor is a ligand for osteoprotegerin/osteoclastogenesis-inhibitory factor and is identical to TRANCE/RANKL. *Proc Natl Acad Sci U S A* 95: 3597–3602, 1998.

Table caption

Table 1: Body weights and muscle mass normalized to body weight of mice. Denervation and/or muscle RANK deletion did not influence body weight. Treatment, but not genotype, reduced EDL and Sol muscle mass normalized to body weight. Data are presented as mean +/- SEM, n=7. The level of significance was set at # $p<0.05$ for treatment (Sham vs Den).

Table 2: Contractile properties of Sol and EDL muscles. Ctr, sham and denervated $RANK^{f/f}$ and $RANK^{mko}$ SOL and EDL muscles were incubated ex vivo and electrically stimulated to record maximal absolute force (P_0) and twitch tension Pt (g). P_0 (g) decreased independently of genotype following denervation. However, muscle RANK deletion prevented the loss of twitch force in denervated EDL muscles. No difference in P_0 and P_t were observed in muscle RANK deletion of control mice. Data are presented as mean +/- SEM, n=7. The level of significance was set at # $p<0.05$ for treatment (Sham vs Den).

Figure caption

Figure 1: RANK expression in skeletal muscles and myotubes. (a) Western blot showing that fully differentiated C2C12 myotubes but not myoblasts express RANK protein. GAPDH is shown as a loading control **(b)** Confocal images showing colocalization of intracellular face of cytoplasmic membrane/sarcolemma dystrophin (green) and RANK (red) in $RANK^{f/f}$ and the absence of RANK in $RANK^{mko}$ EDL muscles. Thymus sections were used as positive controls for RANK immunofluorescence. Omission of primary antibody was used as a negative control. Because non muscle cells in skeletal muscles can also express RANK, confocal images, rather than Western blots, were required to confirm the absence of muscle RANK in $RANK^{mko}$ mice. Bar =100 □m. **(c)** PCR analysis of genomic DNA isolated from Sol muscle, EDL muscle, heart, liver, spleen and kidney showing efficient Cre-mediated recombination of loxP sites in skeletal muscles from $RANK^{mko}$ mice.

Figure 2: Impact of RANK deletion on muscle contractility, fatigue and phenotype. (**a**) Muscle atrophy was significantly more pronounced in denervated $RANK^{mko}$ relative to $RANK^{f/f}$ EDL muscles. (**b**) However, ex vivo force measurements show that RANK ablation preserves the specific force tension of denervated (Den) EDL muscles but not in slow-twitch Sol muscles. (**c**) RANK deletion increases Pt/P_0 ratio in Sol and EDL muscles following denervation. (**d**) Muscle glycolytic fatigue protocol was induced by a train of stimulations (200 ms on: 800 ms off, 50 Hz) until Sol muscles force reach 70% of its initial force. Fatigue time is decreased in denervated muscle but similar between $RANK^{f/f}$ and $RANK^{mko}$ muscles. **(e)** Muscle glycolytic fatigue protocol was induced by a train of stimulations (200 ms on: 800 ms off, 50 Hz) until EDL muscles force reach 50% of its initial force. Sham and denervated $RANK^{mko}$ EDL muscles exhibit increased fatigability compared to sham and denervated $RANK^{f/f}$ EDL muscles. (**f**) Fiber typing of EDL muscle analysis showed that the slow-twitch

fibers were nearly absent in sham *RANK^{mko}* EDL muscles while the proportion of fast-twitch fibers (IIA+IIB+IIX) was significantly increased in denervated *RANK^{mko}* EDL muscles compared to denervated *RANK$^{f/f}$* EDL muscles. The levels of significance were set at * $p<0.05$, ** $p<0.01$, *** $p<0.001$ for genotype (Rank$^{f/f}$ vs Rank^{mko}) or # $p<0.05$ for treatment (Sham vs Den). Data are presented as mean +/- SEM, n = 3-7.

Figure 3: Percentage of type I and II fibers in Sol muscles and proportion of each fiber type expressing SERCA-1a and SERCA-2a in Sol and EDL muscles. (a) As opposed to fast-twitch EDL muscles, no changes in phenotype were observed in sham or denervated RANK$^{f/f}$ and RANK^{mko} in Sol muscles. (**b**) Sham and denervated RANK^{mko} muscles exhibited a lower proportion of fast-twitch fibers expressing SERCA-1a and a higher proportion of fast-twitch fibers expressing SERCA-2a. The levels of significance were set at * $p<0.05$, ** $p<0.01$, *** $p<0.001$ for genotype (Rank$^{f/f}$ vs Rank^{mko}) or # $p<0.05$ for treatment (Sham vs Den). Data are presented as mean +/- SEM, n = 6-8.

Figure 4: Total calcium content, SERCA activity and calcium protein contents in RANK$^{f/f}$ and RANK^{mko} EDL muscles. (**a-c**) [CaT] was decreased in sham RANK^{mko} EDL muscles relative to sham RANK$^{f/f}$ EDL muscles but increased sharply in denervated RANK^{mko} EDL muscles. **(d)** Western blots show that SERCA-1a content is reduced while SERCA-2a content is increased following denervation. No changes in calsequestrin content were observed, but Stim1 content increased markedly in denervated RANK^{mko} EDL muscles. **(e)** SERCA Ca^{2+}-dependent ATPase activity was assessed in muscle homogenates from sham and denervated RANK$^{f/f}$ and RANK^{mko} EDL muscles over Ca^{2+} concentrations ranging from pCa 7.4 to pCa5.0 (**f**) maximal ATPase activity (Vmax) and (**g**) pCa value required to elicit 50% of maximal activity (pCa50). The levels of significance were set at * $p<0.05$, ** $p<0.01$,

*** p<0.001 for genotype ($Rank^{f/f}$ vs $Rank^{mko}$) or # p<0.05 for treatment (Sham vs Den). Data are presented as mean +/- SEM, n = 3-7.

Figure 5: SERCA Ca^{2+}-dependent ATPase parameters from sham and denervated $RANK^{f/f}$ and $RANK^{mko}$ in Sol muscles. Denervation induced a significant reduction of (a) SERCA Ca^{2+} dependent ATPase activity and Vmax (b) maximal ATPase activity (Vmax) (c) pCa value required to elicit 50% of maximal activity (pCa50) were similar between control and experimental Sol muscles. The level of significance between genotype ($Rank^{f/f}$/$Rank^{mko}$) was set at * p<0.05, ** p<0.01, *** p<0.001 and set at # p<0.05 between treatment (Sham/Den). Data are presented as mean +/- SEM, n = 3-7.

Figure 6: Schematic representation of RANK/RANKL/OPG pathway as common regulator of bone and muscle cells. In osteoclast, RANK/RANKL interaction regulates osteoclastogenesis and/or cell apoptosis through modulation of SERCA activity, Ca^{2+} oscillation, Ca^{2+}-calcineurin-NFAT and NF-kB pathways. Muscle cells also express RANK and RANK/RANKL interaction is an important regulator of SERCA activity, calcium storage in fast-twitch EDL muscles. These results highlight the importance of a common signalling pathway opening potentially new treatment for both skeletal muscle and bone.

Table 1

	Mice			
	$Sham^{f/f}$	$Den^{f/f}$	$Sham^{mko}$	Den^{mko}
Body weight (g)	24.7 ± 0.8	24.3 ± 0.7	23.8 ± 1.4	24.5 ± 1.9
EDL muscle weight / Body weight	0,34 ± 0,05	0,28 # ± 0,02	0,38 ± 0,04	0,25 # ± 0,04
Sol muscle weight / Body weight	0,29 ± 0,04	0,24 # ± 0,03	0,26 ± 0,03	0,23 # ± 0,04

Table 2

	Sol						EDL					
	$Ctr^{f/f}$	$Sham^{f/f}$	$Den^{f/f}$	Ctr^{mko}	$Sham^{mko}$	Den^{mko}	$Ctr^{f/f}$	$Sham^{f/f}$	$Den^{f/f}$	Ctr^{mko}	$Sham^{mko}$	Den^{mko}
P_0 (g)	26.6 ± 1.2	26.1 ± 0.6	19.6# ± 0.4	26.9 ± 1.5	25.6 ± 1.4	18.1# ± 1.8	33.5 ± 1.7	33.1 ± 1.6	21.3# ± 1.4	32.7 ± 1.8	33.5 ± 1.3	22.1# ± 1.4
Pt (g)	3.8 ± 0.6	4.3 ± 0.2	4.2 ± 0.3	4.8 ± 0.5	4.3 ± 0.4	4.9 ± 0.4	7.1 ± 0.6	7.5 ± 0.8	5.6# ± 0.5	5.3 ± 0.6	5.8 ± 0.8	6.2 ± 0.4

Figure 1

a)

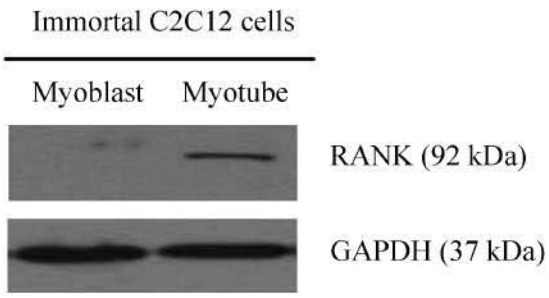
Immortal C2C12 cells
Myoblast
Myotube
RANK (92 kDa)
GAPDH (37 kDa)

b)

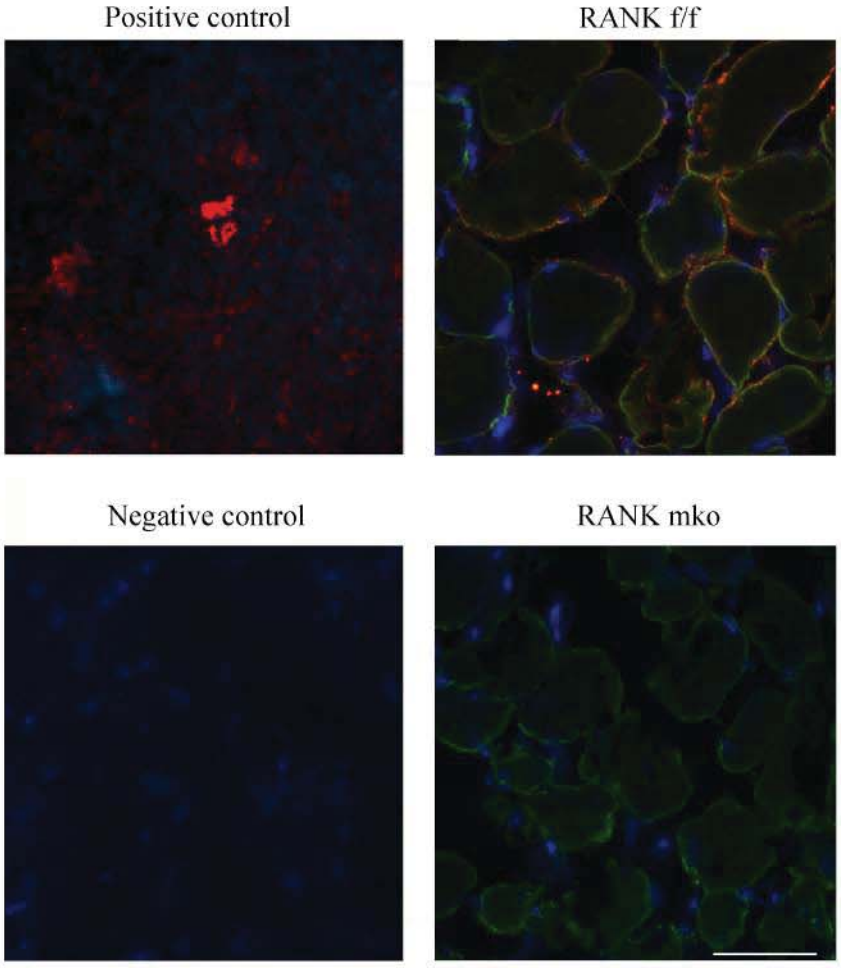
Positive control
RANK f/f
Negative control
RANK mko

c)

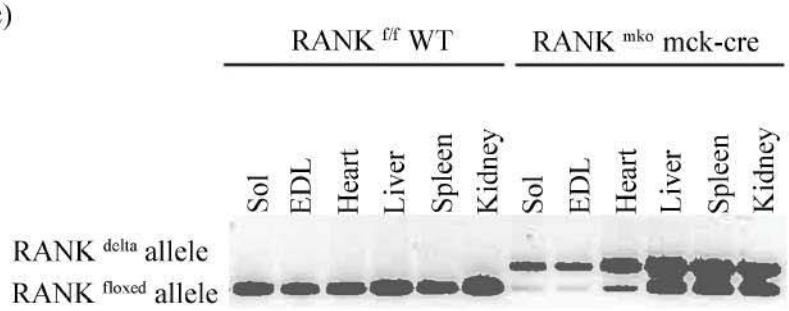
RANK f/f WT
RANK mko mck-cre
Sol
EDL
Heart
Liver
Spleen
Kidney
Sol
EDL
Heart
Liver
Spleen
Kidney
RANK delta allele
RANK floxed allele

Figure 2

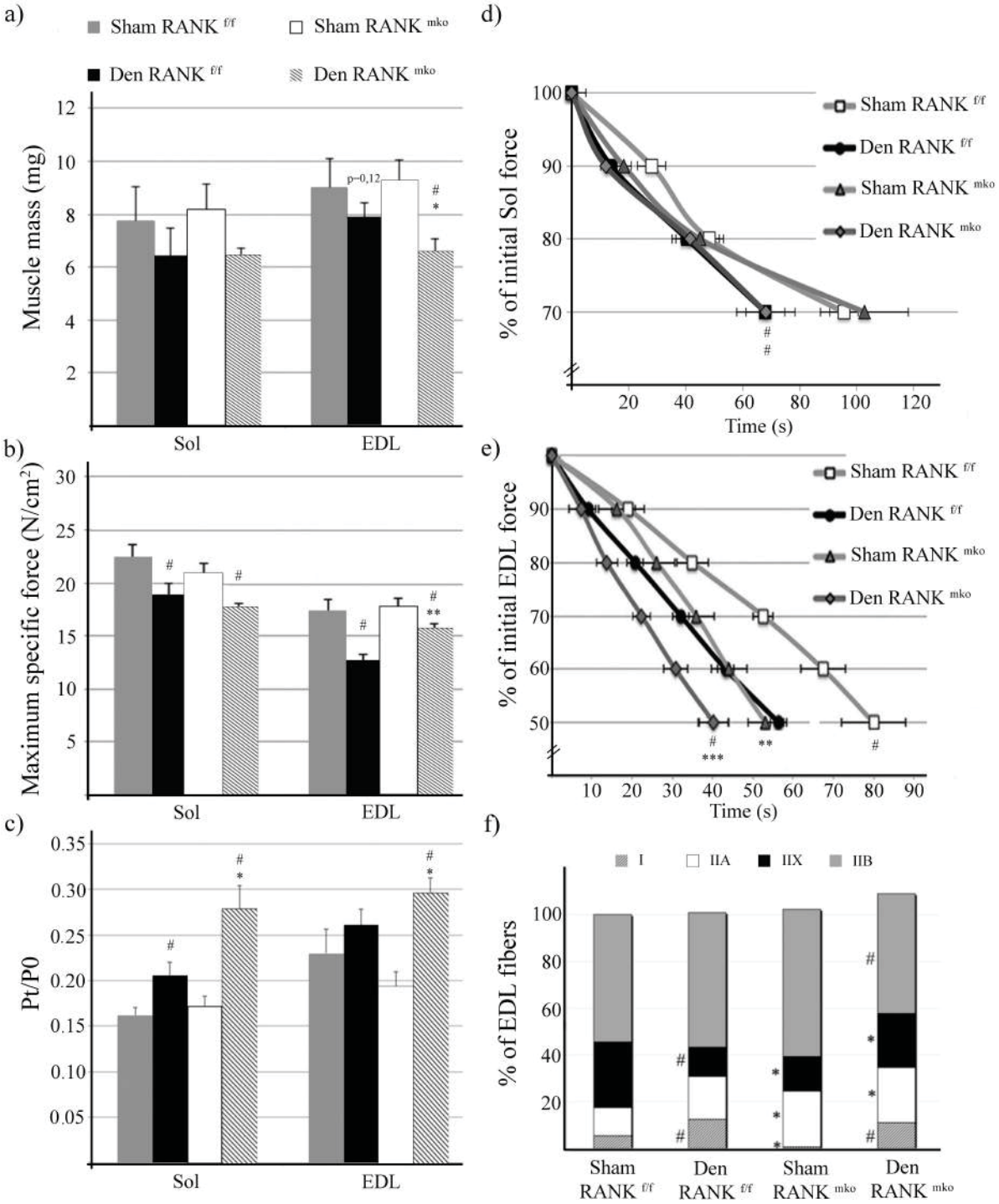
a)
Sham RANK f/f
Sham RANK mko
Den RANK f/f
Den RANK mko
Muscle mass (mg)
p=0,12
Sol
EDL
b)
Maximum specific force (N/cm²)
Sol
EDL
c)
Pt/P0
Sol
EDL
d)
% of initial Sol force
Time (s)
e)
% of initial EDL force
Time (s)
f)
I
IIA
IIX
IIB
% of EDL fibers
Sham RANK f/f
Den RANK f/f
Sham RANK mko
Den RANK mko

Figure 3

a)

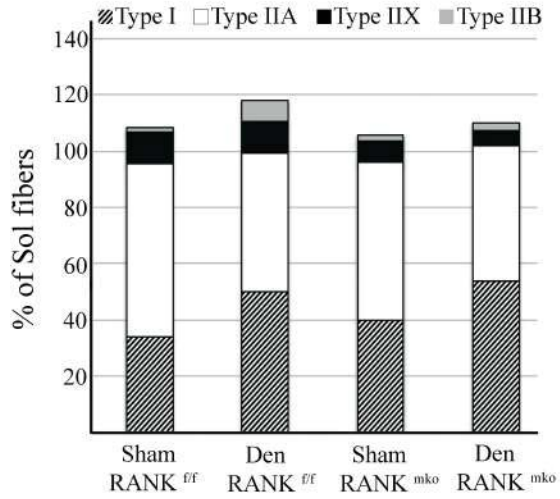
Type I
Type IIA
Type IIX
Type IIB
% of Sol fibers
140
120
100
80
60
40
20
Sham RANK f/f
Den RANK f/f
Sham RANK mko
Den RANK mko

b)

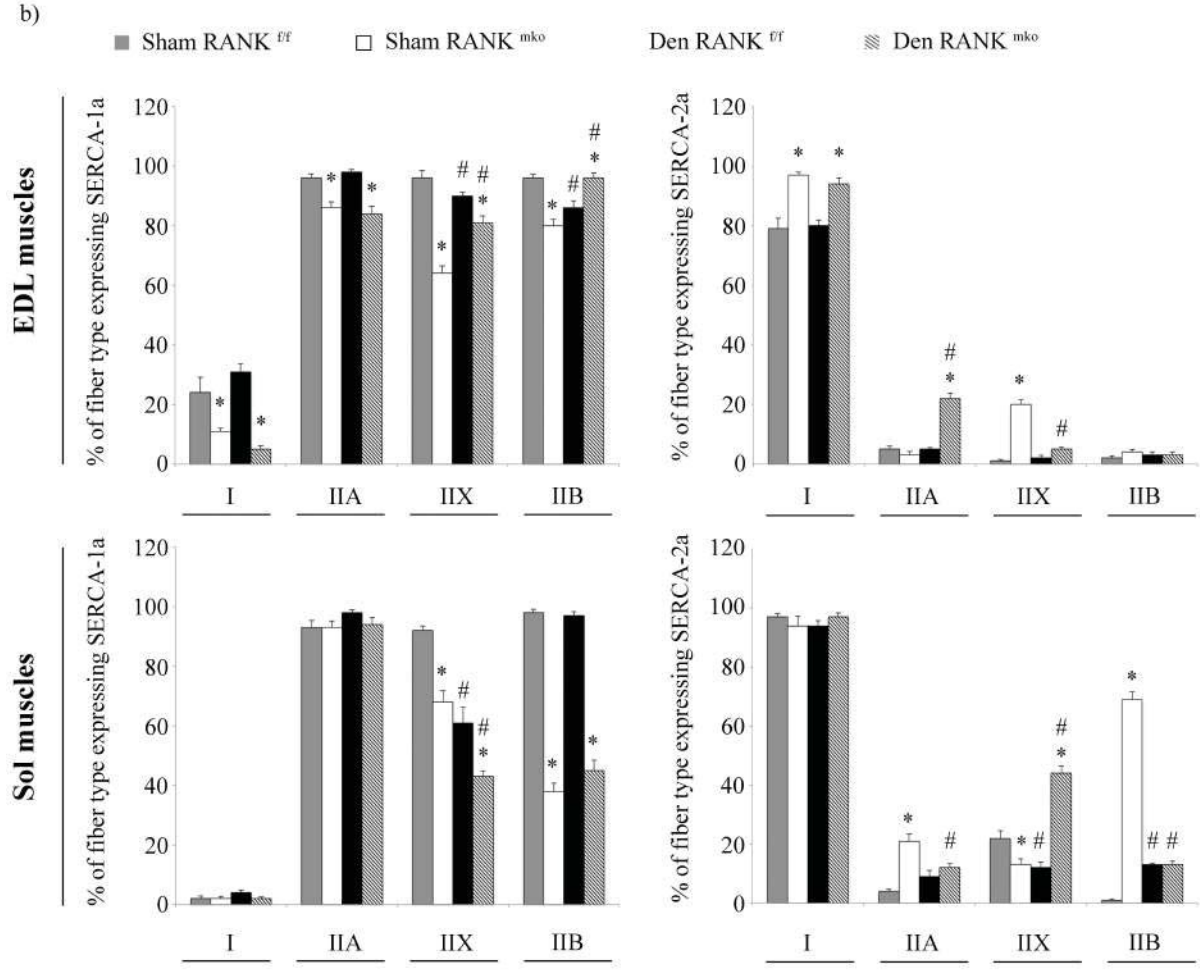
Sham RANK f/f
Sham RANK mko
Den RANK f/f
Den RANK mko
EDL muscles
Sol muscles
% of fiber type expressing SERCA-1a
% of fiber type expressing SERCA-2a
I
IIA
IIX
IIB

Figure 4

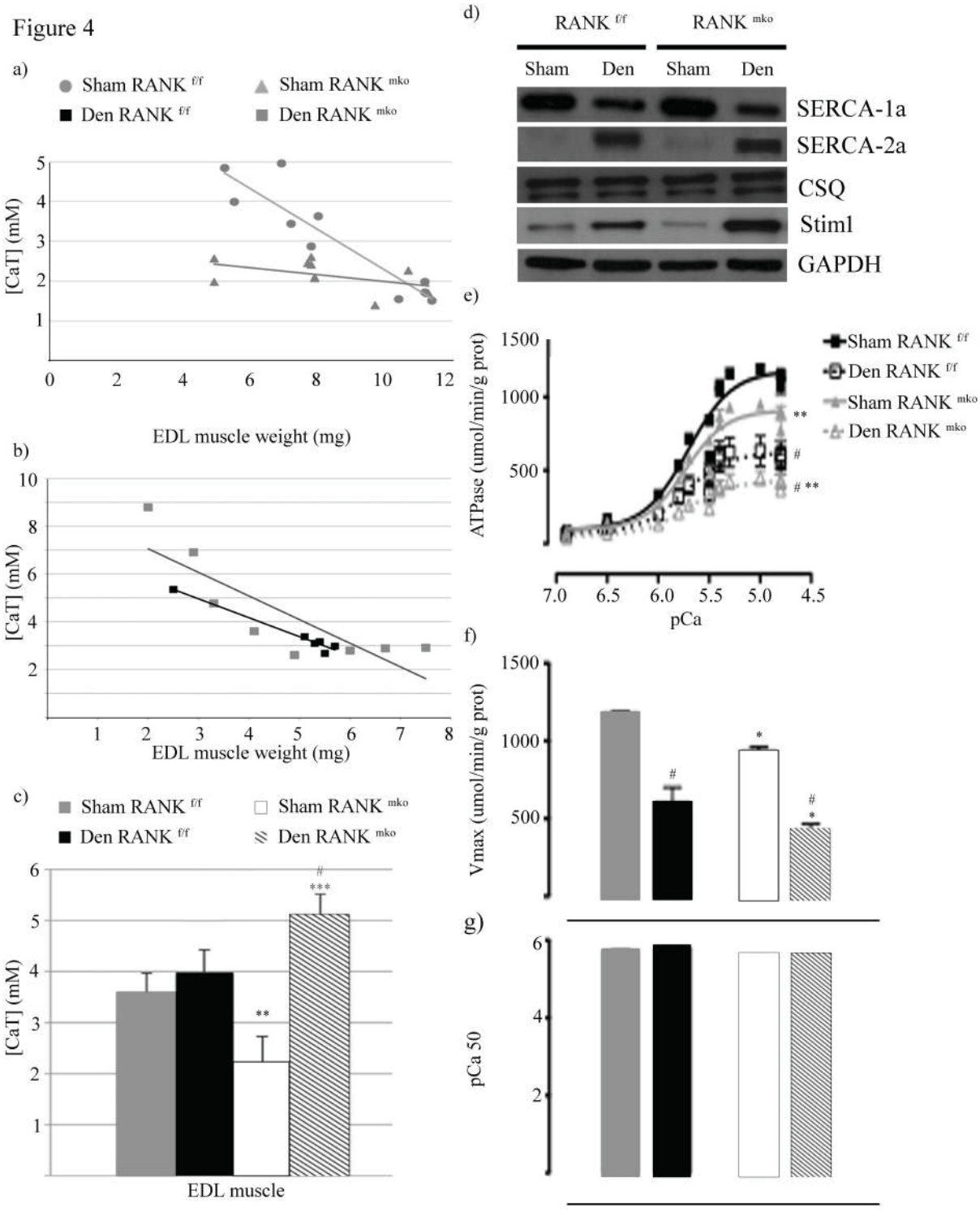
a)
Sham RANK f/f
Sham RANK mko
Den RANK f/f
Den RANK mko
[CaT] (mM)
EDL muscle weight (mg)
b)
[CaT] (mM)
EDL muscle weight (mg)
c)
Sham RANK f/f
Sham RANK mko
Den RANK f/f
Den RANK mko
[CaT] (mM)
EDL muscle
d)
RANK f/f
RANK mko
Sham
Den
Sham
Den
SERCA-1a
SERCA-2a
CSQ
Stim1
GAPDH
e)
Sham RANK f/f
Den RANK f/f
Sham RANK mko
Den RANK mko
ATPase (umol/min/g prot)
pCa
f)
Vmax (umol/min/g prot)
g)
pCa 50

Figure 5

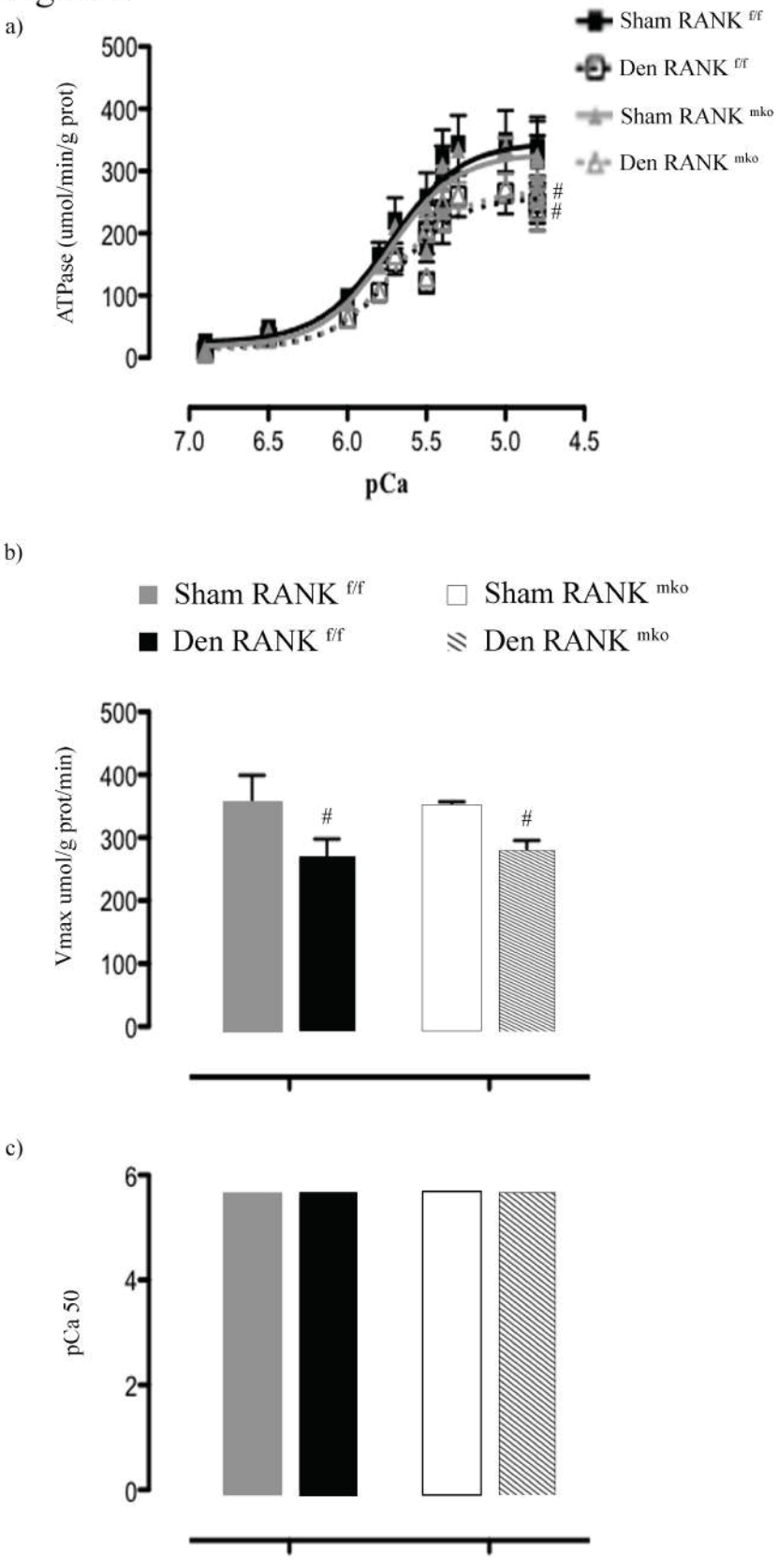
a)
Sham RANK f/f
Den RANK f/f
Sham RANK mko
Den RANK mko
ATPase (umol/min/g prot)
500
400
300
200
100
0
#
#
7.0
6.5
6.0
5.5
5.0
4.5
pCa
b)
Sham RANK f/f
Sham RANK mko
Den RANK f/f
Den RANK mko
Vmax umol/g prot/min)
500
400
300
200
100
0
#
#
c)
pCa 50
6
4
2
0

Figure 6

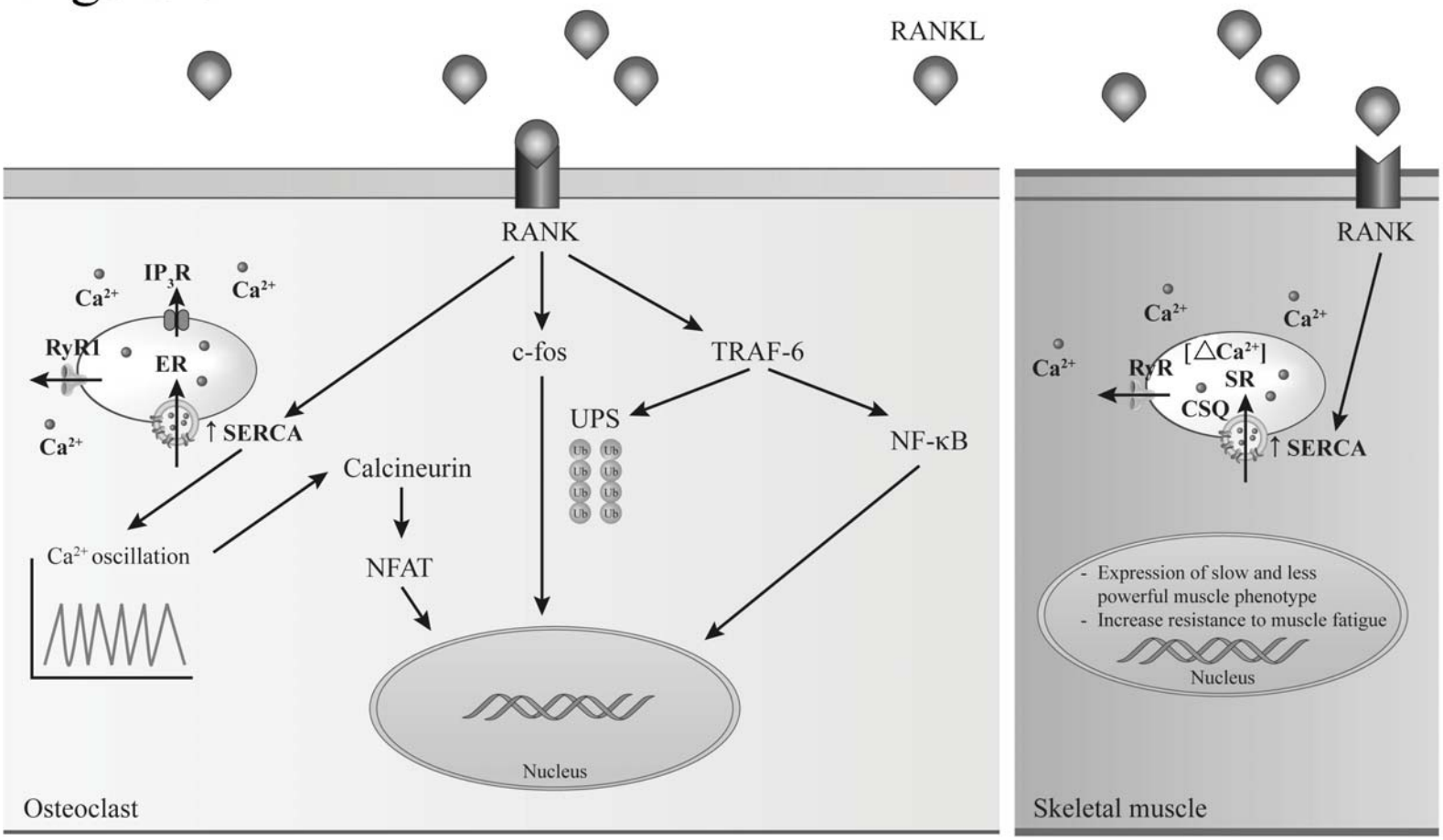
RANKL
RANK
IP3R
Ca2+
Ca2+
RyR1
ER
Ca2+
↑ SERCA
c-fos
TRAF-6
UPS
NF-κB
Calcineurin
Ca2+ oscillation
NFAT
Nucleus
Osteoclast
RANK
Ca2+
Ca2+
Ca2+
[△Ca2+]
RyR
SR
CSQ
↑ SERCA
- Expression of slow and less powerful muscle phenotype
- Increase resistance to muscle fatigue
Nucleus
Skeletal muscle